

Passive shape control of force-induced harmonic lateral vibrations for laminated piezoelectric Bernoulli-Euler beams-theory and practical relevance

J. Schoeftner* and H. Irschik

*Institute of Technical Mechanics, Johannes Kepler University of Linz, A-4040 Linz,
Altenbergerstr.69, Austria*

(Received December 30, 2010, Accepted April 21, 2011)

Abstract. The present paper is devoted to vibration canceling and shape control of piezoelectric slender beams. Taking into account the presence of electric networks, an extended electromechanically coupled Bernoulli-Euler beam theory for passive piezoelectric composite structures is shortly introduced in the first part of our contribution. The second part of the paper deals with the concept of passive shape control of beams using shaped piezoelectric layers and tuned inductive networks. It is shown that an impedance matching and a shaping condition must be fulfilled in order to perfectly cancel vibrations due to an arbitrary harmonic load for a specific frequency. As a main result of the present paper, the correctness of the theory of passive shape control is demonstrated for a harmonically excited piezoelectric cantilever by a finite element calculation based on one-dimensional Bernoulli-Euler beam elements, as well as by the commercial finite element code of ANSYS using three-dimensional solid elements. Finally, an outlook for the practical importance of the passive shape control concept is given: It is shown that harmonic vibrations of a beam with properly shaped layers according to the presented passive shape control theory, which are attached to a resistor-inductive circuit (*RL*-circuit), can be significantly reduced over a large frequency range compared to a beam with uniformly distributed piezoelectric layers.

Keywords: piezoelectric modeling of beams; shape control; passive vibration control; design optimization of slender piezoelectric beams; electric network; vibration damping with *RL*-circuit.

1. Introduction

The present paper deals with dynamic shape control of electromechanically coupled slender beams which consist of piezoelectric layers attached on both sides of a substrate. The electrodes of the upper and lower layers are connected by electric circuits and therefore such systems belong to the class of passive piezoelectric structures, as opposed to actuated smart structures, where the voltage difference over the electrodes is prescribed by an external power supply. In contrast to the existing literature on quasi-static and dynamic shape control, where a spatial distribution of an actuating control agency is externally applied to a structure in order to achieve a desired spatial displacement field, we intend to eliminate lateral vibrations for passive, non-actuated smart beam-type structures. The notion passive shape control here means that this objective is realized by optimally tuned

*Corresponding Author, Researcher, E-mail: juergen.schoeftner@lcm.at

electric networks and by using spatially distributed piezoelectric layers. The modeling of the physical interaction of piezoelectric materials and elastic structures has gained importance in engineering practice. These systems are called smart systems: piezoelectricity closes the gap between mechanical and electric fields by taking advantage of both the direct and the indirect piezoelectric effect. Piezoelectric patches are embedded in flexible systems in order to reduce vibrations utilizing optimal control algorithms. Some recently published examples concerning the modeling of electromechanically coupled composite beams can be found in Zhou *et al.* (2005), Krommer and Irschik (2002) and Krommer (2001). In Zehetner and Irschik (2008) and Zehetner (2010), the static and dynamic stability of piezoelectric laminated beams is investigated using a Bernoulli-Euler-v. Karman beam theory. The thermal analogy and the strain induced potential concept to model piezoelectric structures are extensively discussed in Benjeddou (2009). Feedback control of smart systems based on optimal control laws and the choice of optimal locations of piezoelectric patches are treated in Behesthi-Aval and Lezgy-Nazargah (2010) and Gabbert *et al.* (2007). The notion shape control has been first introduced by Hafka and Adelman (1985) presenting an analytical computation of the temperature field of a supporting structure to minimize distortions of space structures from their original shape. Vibrations of rotary wings are reduced in Nitzsche and Breitbach (1994), where smart structures were used to construct geometric modal filters that are able to control the critical modes. The experimental setup presented in Nader (2007) verifies the theoretical result of shape control for beam-type structures: if the smart actuation is the negative quasi-static bending moment due to transient imposed forces, the total vertical deflection is zero. For a cantilever beam with prescribed boundary motion, base-excited vibrations by using a discretized parabolic distribution of actuated piezoelectric patches were annihilated. For clamped circular plates with a spatially constant force loading, flexural vibrations were nullified using an analytic solution derived by the Kirchhoff theory for thin plates, which was validated by a three dimensional coupled finite element computation, see Nader *et al.* (2003). In Irschik *et al.* (2001) and Irschik *et al.* (2003) the main goal was to find spatially distributed self-sensing layers that are perfectly glued on a substrate in order to cancel vibrations of beams for various boundary conditions. Further contributions on shape control of subsections of flexible structures and on the reduction of the high-voltage level of the actuated patches were published in Krommer (2005) and Yu *et al.* (2009). A dynamic shape control problem is solved in Irschik and Pichler (2004), where force-induced vibrations are exactly eliminated by seeking a transient distribution of actuation stress. The control of deformations in linear elastic bodies is treated in Ziegler (2005). A review of static and dynamic shape control by piezoelectric actuation is given in Irschik (2002). Shape control belongs to the class of so-called inverse problems where stress resultants and couples are calculated in order to obtain a desired displacement field. Their solution either may not exist or is not unique. E.g. consider a clamped-clamped slender beam with a constant or a linear distribution of an actuated piezoelectric layer. The beam will not experience lateral deflections if an electric voltage is applied on the upper and lower electrodes of the piezoelectric actuator, see Hubbard and Burke (1992), Irschik *et al.* (2003) and Irschik *et al.* (1998). Hence, adding constant or linear shape distributions of piezoelectric actuators do not change the solution. Such shapes are known as nil-potent shape functions.

The present paper represents an extension of our previous contributions Schoeftner and Irschik (2009) and Schoeftner and Irschik (2010), in which we have transmitted the concept of shape control to passive piezoelectric slender beams. Our intention in Schoeftner and Irschik (2010) has been to find spatial distributions of the piezoelectric layers, being attached to a substrate beam and being connected to optimally tuned electric networks, in order to perfectly cancel deformations of

slender beams with arbitrary transverse force loading and arbitrary boundary conditions. The case of a cantilever with a uniform force loading was treated in Schoeftner and Irschik (2009), where we have obtained an analytical solution for passive shape control. In the present work, the necessary and sufficient conditions of passive shape control are validated by means of three-dimensional electromechanically coupled finite element computations with ANSYS 11.0. Particularly, the following problems are treated and the corresponding solutions are justified: According to our theory, a cantilever, which is excited by a harmonic triangular force load along the beam axis and an end moment, does not vibrate, if the spatially varying layers and the network are optimally designed for a specific target frequency. Additionally, we give a contribution on the optimal and robust design of passive piezoelectric structures, which is important for practical applications: We compare the vibrations of a beam with properly shaped layers to those of a beam with uniformly distributed layers. Both configurations are attached to inductive-resistive networks (RL) and the maximum magnitude of the tip deflection is minimized around the first natural frequency of the beam by varying the impedances of the circuit. It is found that the vibrations with a uniformly distributed layer are about one third larger than those of a beam whose piezoelectric parts are shaped according to the present shape control theory.

2. Lateral equation of motion of slender composite piezoelectric beams interacting with electric circuits

This section presents the governing equations of motion for bending of a slender, three layer piezoelectric beam shown in Fig. 1. For a thin beam, the predominating stress and electric displacement components are the axial stress σ_{xx} and the electric displacement in thickness direction D_z , see Irschik *et al.* (2003) and Krommer (2001). Consequently, the reduced form of the piezoelectric constitutive relations (e.g., PZT-5A) is written as

$$\sigma_{xx}^k = \tilde{C}_{11}^k \epsilon_{xx}^k - \tilde{e}_{31}^k E_z^k, \quad D_z^k = \tilde{e}_{31}^k \epsilon_{xx}^k + \tilde{\kappa}_{33}^k E_z^k \quad (1)$$

where \tilde{C}_{11}^k , \tilde{e}_{31}^k and $\tilde{\kappa}_{33}^k$ denote the effective values of the Young modulus, the piezoelectric transverse coefficient and the strain-free dielectric constant, respectively. The tracer k stands for substrate, lower and upper layer or piezo (s, l, u or p). The tracer p is used, if the physical values are the same for both the upper and lower layer. The transformation rules and the dependency of the effective values on piezoelectric material tensors are explained in Krommer and Irschik (2002). The axial mechanical

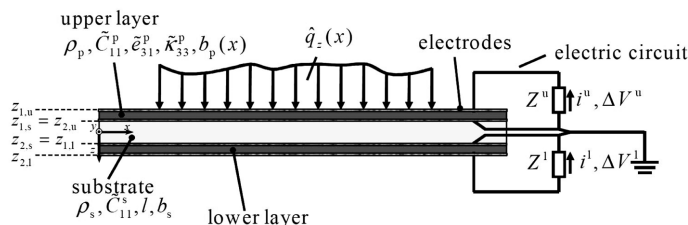


Fig. 1 Laminated beam with electroded piezoelectric upper and lower layers which are connected to electric circuits. The width of the substrate b_s is constant, the width of the layers is a function of the axial direction $b_p(x)$.

strain ε_{xx} in Eq. (1) and the electric field E_z are given as ($\partial(\cdot)/\partial z := (\cdot)_{,z}$)

$$\varepsilon_{xx}(x, z) = -zw_{0,xx}(x), \quad E_z = V_{,z} \quad (2)$$

In the following, the Laplace transform is used since it is assumed that the external forces are time-harmonic. Hence, the hat-symbol characterizes variables in the Laplace domain:

$$\hat{f}(x, s) = \mathcal{L}\{f(x, t)\} \quad (3)$$

If D'Alembert's principle is applied, see Ziegler (1995) and Krommer (2001),

$$\int_V \hat{\sigma}_{xx} \delta \hat{\varepsilon}_{xx} dV + \int_V s^2 \rho \hat{w}_0 \delta \hat{w}_0 dV = \int_V q_z \delta \hat{w}_0 dV$$

the electromechanically coupled boundary value problem describing the transverse motion of a smart passive beam can be derived in the Laplace domain, taking into consideration of Kirchhoff's voltage rule, the constitutive piezoelectric relations in Eq.(1) and the geometrical relation in Eq. (2)

$$s^2 M_w \hat{w}_0 + (K_M w_{0,xx})_{,xx} = \sum_{k=u,l} \frac{\tilde{e}_{31}^k}{2} \Delta \hat{V}^k (z_{2,k} + z_{1,k}) b_{k,xx}(x) + \hat{q}_z(x) \quad (5)$$

where the inertia M_w , the mechanical and the piezoelectric bending stiffness $K_M = K_{M, mech} = K_{M, el}$ are given as

$$M_w(x) = \sum_{k=s,u,l} \int_{z_{1,k}}^{z_{2,k}} \rho_k(x) dA_k \quad (6)$$

$$K_M(x) = \sum_{k=s,u,l} \tilde{C}_{11}^k b_k(x) \frac{z_{2,k}^3 - z_{1,k}^3}{3} + \sum_{k=u,l} \frac{\tilde{e}_{31}^{2,k} (z_{2,k} - z_{1,k})^3 b_k(x)}{12 \tilde{\kappa}_{33}^k}$$

The voltage drop of the lower and upper circuit is given by

$$\Delta \hat{V}^k = -\tilde{e}_{31}^k s \left(\frac{\int_0^l \hat{w}_{0,xx} b_k(x) dx (z_{2,k} + z_{1,k})}{2 [s C_p^k + (Z^k)^{-1}]} \right) \quad \text{for } k = l, u. \quad (7)$$

For a more detailed derivation and a discussion of the fundamental assumptions, see Schoeftner and Irschik (2009) and Krommer and Irschik (2002). The variables C_p^k and Z^k are the capacitance of the piezoelectric lower and upper layer, and the impedance of the electric network, respectively. For our further considerations, it is useful to split the bending moment and the shear force into a piezoelectric-mechanical and an electrical part

$$\hat{M}(x) = \hat{M}_{mech}(x) + \hat{M}_{el}(x) \quad (8)$$

$$\hat{Q}(x) = \hat{M}_{,x}(x) = \hat{Q}_{mech}(x) + \hat{Q}_{el}(x)$$

with

$$\begin{aligned}
\hat{M}_{mech}(x) &= -(K_M w_{0,xx}) \\
\hat{M}_{el}(x) &= \sum_{k=u,1} \tilde{e}_{31}^k \Delta V^k (z_{2,k} + z_{1,k}) b_k(x) / 2 \\
\hat{Q}_{mech}(x) &= -(K_M w_{0,xx})_{,x} \\
\hat{Q}_{el}(x) &= \sum_{k=u,1} \tilde{e}_{31}^k \Delta \hat{V}^k (z_{2,k} + z_{1,k}) b_{k,x}(x) / 2.
\end{aligned} \tag{9}$$

3. Necessary conditions for exact vibration canceling of passive smart beams

For the further calculation we assume that the impedance Z^k is equal for the lower and upper electric network and that the midplane is a symmetry plane; then

$$\begin{aligned}
z_{1,l} = -z_{2,u} = z_{1,p}, \quad z_{2,l} = -z_{1,u} = z_{2,p}, \quad b_l(x) = b_u(x) = b_p(x), \\
\tilde{e}_{31}^l = \tilde{e}_{31}^u = \tilde{e}_{31}^p, \quad \tilde{\kappa}_{33}^l = \tilde{\kappa}_{33}^u = \tilde{\kappa}_{33}^p, \quad \tilde{C}_{11}^l = \tilde{C}_{11}^u = \tilde{C}_{11}^p, \\
Z^l = Z^u = Z
\end{aligned} \tag{10}$$

must hold for the material parameters and the geometric dimensions of the piezoelectric layers. Hence, for the voltage differences of the upper and lower layer follows from Eq. (7)

$$\Delta \hat{V} = \Delta \hat{V}^l = -\Delta \hat{V}^u \tag{11}$$

and we can neglect the tracer for the voltage in the following. Assuming homogeneous kinematic and/or dynamic boundary conditions, the main idea of the total annihilation of lateral vibrations $\hat{w}_0(x)$ follows by equating to zero the right-hand side of Eq. (5), which yields, if the electrical bending moment $\hat{M}_{el}(x)$ in Eq.(9) is considered

$$-\hat{M}_{el,xx}(x) = -\tilde{e}_{31}^p \Delta \hat{V} (z_{2,p} + z_{1,p}) b_{p,xx}(x) = \hat{q}_z(x) \tag{12}$$

It is obvious from Eqs. (12) and (7), that the spatial dependency of the electrical bending moment is given by the shape $b_p(x)$ of the layers only and that the amplitude is affected by the impedance of the circuit Z . In the next sections, two conditions are presented (the impedance matching and the shaping condition) in order to satisfy Eq.(12).

3.1. Impedance matching condition

Since our objective is to nullify the displacement $\hat{w}_0(x)$, the right-hand side of Eq. (5) has to vanish. The voltage drop, given by Eq. (7), is proportional to the transverse deflection, and can be only non-zero if also the denominator vanishes. This yields to the following impedance matching condition

$$Z = -\frac{1}{sC_p} \tag{13}$$

If an *RLC* serial circuit (consisting of a resistor R , an inductance L and a capacitor C) is considered, where $Z = Ls + R + (sC_p)^{-1}$ holds, one may substitute $s = j\omega$ for the complex Laplace variable. Consequently, two equations for the imaginary and the real part of Eq. (13) are found in the form

$$R = 0, \quad L = \frac{C_p + C}{\omega^2 C_p C} \quad (14)$$

The impedance matching condition Eq. (14) states that the Ohm's resistance R has to vanish and that the uncoupled electric eigenfrequency of the network must be equal to the driving frequency ω of the external forces.

3.2. Shaping condition

One can conclude that the right hand side of Eq. (5) will not disappear in general, if the piezoelectric layer is not properly shaped. So the second spatial derivative of the width of the layers must be proportional to the external force loading

$$\hat{q}_z(x) \propto b_{p,xx}(x) \quad (15)$$

For instance, it is assumed that the external mechanical load consists of a distributed load $\hat{f}_z(x)$, a concentrated force \hat{F}_0 and a concentrated moment \hat{M}_0 acting at the locations x_{F_0} and x_{M_0}

$$\hat{q}_z(x) = \hat{f}_z(x) + \hat{F}_0 \delta(x - x_{F_0}) + \hat{M}_0 \delta_{,x}(x - x_{M_0}). \quad (16)$$

Integrating this relation twice from 0 to x and using Eq. (15), the width $b_p(x)$ of the piezoelectric layers is determined by the shaping condition

$$\begin{aligned} \int_0^x \int_0^x \hat{q}_z(x) dx dx &= \int_0^x \int_0^x \hat{f}_z(x) dx dx + \hat{F}_0 H(x - x_{F_0})(x - x_{F_0}) \\ &+ \hat{M}_0 H(x - x_{M_0}) + G_{z,1}x + G_{z,2} \propto b_p(x) \end{aligned} \quad (17)$$

where the integration constants $G_{z,1}$ and $G_{z,2}$ still remain unknown. The boundary-value problem of a Bernoulli-Euler beam can be solved if four boundary conditions are given, which must be trivial, in order to nullify the deflection. Kinematic boundary condition fulfill this criterion in a trivial way

$$\hat{w}_0(x^*) = 0 \quad \text{and/or} \quad w_{0,x}(x^*) = 0 \quad \text{at} \quad x^* = 0, l. \quad (18)$$

For dynamic boundary conditions

$$\hat{M}(x^*) = 0 \quad \text{and/or} \quad \hat{Q}(x^*) = M_{,x}(x^*) \quad \text{at} \quad x^* = 0, l. \quad (19)$$

hold. Splitting up the bending moment and/or the shear force into mechanical and electrical parts, see Eqs. (8) and (9), the latter ones will disappear by all means if the width and/or the first spatial derivative of the width vanish at the dynamic boundary conditions

$$\begin{aligned} \hat{M}_{el}(x^*) = \tilde{e}_{31}^p \Delta \hat{V}(z_{2,p} + z_{1,p}) b_p(x^*) = 0 &\Leftrightarrow b_p(x^*) = 0 \\ \hat{Q}_{el}(x^*) = \tilde{e}_{31}^p \Delta \hat{V}(z_{2,p} + z_{1,p}) b_{p,x}(x^*) = 0 &\Leftrightarrow b_{p,x}(x^*) = 0 \\ &\text{at} \quad x^* = 0, l. \end{aligned} \quad (20)$$

Consequently, it follows from Eqs.(19) and (20) that the mechanical portions of the bending moment $\hat{M}_{\text{mech}}(x^*)$ and the shear forces $\hat{Q}_{\text{mech}}(x^*)$, which depend on the second and third derivative of $\hat{w}_0(x)$ with respect to x (Eq. (9)), also vanish. We can conclude that the two integration constants $G_{z,1}$ and $G_{z,2}$ in Eq. (17) and the shape of the layers, are only uniquely determined, if the beam is statically determinate (i.e., if two dynamic and two kinematic boundary conditions are present). If only one or none dynamic boundary conditions are present (i.e., if the beam is statically indeterminate), the shape of the layers is not unique and so-called nil-potent shape functions exist, see Irschik *et al.* (2003) or Schoefner and Irschik (2010). In the next subsection, we will prove that if the impedance matching and the shaping condition are fulfilled, these conditions are not only necessary, but also sufficient conditions for the vibration canceling problem of slender beams.

4. Proof that necessary conditions are also sufficient conditions for passive vibration canceling

In this section we exemplarily show for a cantilever beam excited by an arbitrary harmonic load that the above-derived conditions are necessary and also sufficient. If the proportionality sign in Eq. (15) is replaced by the equality sign, the shaping condition can be rewritten as

$$\hat{q}_z(x) = p_z b_{p,xx}(x) \quad (21)$$

where p_z is a proportionality factor that is related to the maximum possible width of the beam configuration, see section 5 below. If Eq. (21) and the voltage drop Eq. (7) are inserted into Eq. (5), then

$$s^2 M_w \hat{w}_0 + (K_M \hat{w}_{0,xx})_{,xx} = \hat{q}_z \underbrace{\left(1 - \frac{P_z}{p_z} \int_0^l w_{0,xx} b_p(x) dx \right)}_{\text{constant function}} \quad (22)$$

is obtained, where P_z is defined as

$$P_z = \frac{s \tilde{e}_{31}^p (z_{2,p} + z_{1,p})^2}{2 [s C_p + Z^{-1}]} \quad (23)$$

The general solution of Eq.(22) can be found in the form

$$\hat{w}_0(x) = \sum_{j=1}^5 A_{w,j} \hat{w}_j(x), \quad (24)$$

where \hat{w}_1 , \hat{w}_2 , \hat{w}_3 , and \hat{w}_4 are the normalized fundamental solutions of the corresponding homogeneous differential equation and \hat{w}_5 is the inhomogeneous solution due to the vertical load $\hat{q}_z(x)$ for a short-circuited piezoelectric beam, called the auxiliary problem

$$Z = 0 \Rightarrow P_z = 0: \quad s^2 M_w \hat{w}_0 + (K_M \hat{w}_{0,xx})_{,xx} = \hat{q}_z(x) \quad (25)$$

The coefficients $A_{w,1}$, $A_{w,2}$, $A_{w,3}$, $A_{w,4}$ and $A_{w,5}$ can be computed by inserting Eq. (24) into the following linear system of equations, where the first four equations represent the kinematic and dynamic boundary conditions of the clamped-free beam, and the last equation is the solution for the inhomogeneous part of the

differential equation (22)

$$\begin{aligned}
 \hat{w}_0(0) &= 0, \\
 \hat{w}_{0,x}(0) &= 0, \\
 \hat{Q}(l) &= - \left[K_M(l) \sum_{j=1}^5 A_{w,j} \hat{w}_{j,xx}(l) \right]_{,x} - P_z b_{p,x}(l) \int_0^l \sum_{j=1}^5 A_{w,j} \hat{w}_{j,xx}(x) b_p(x) dx = 0, \\
 \hat{M}(l) &= -K_M(l) \sum_{j=1}^5 A_{w,j} \hat{w}_{j,xx}(l) - P_z b_p(l) \int_0^l \sum_{j=1}^5 A_{w,j} \hat{w}_{j,xx}(x) b_p(x) dx = 0, \\
 A_{w,5} \left[s^2 M_w \hat{w}_5 + (K_M \hat{w}_{5,xx})_{,xx} \right] &= \hat{q}_z \left[1 - \frac{P_z}{P_z} \int_0^l \sum_{j=1}^5 A_{w,j} \hat{w}_{j,xx}(x) b_p(x) dx \right]
 \end{aligned} \tag{26a-e}$$

Demanding that the shape and the gradient of the layers are zero at $x=l$, where the dynamic boundary conditions hold (free end), see Eq. (20)

$$\begin{aligned}
 b_p(l) &= 0 \Leftrightarrow \hat{M}_{el}(l) = 0 \\
 b_{p,x}(l) &= 0 \Leftrightarrow \hat{Q}_{el}(l) = 0
 \end{aligned} \tag{27}$$

the electrical part of the bending moment and shear force are not present. Taking into account the inhomogeneous solution $\hat{w}_5(x)$ of the auxiliary problem Eq. (25)

$$s^2 M_w \hat{w}_5 + (K_M \hat{w}_{5,xx})_{,xx} = \hat{q}_z(x) \tag{28}$$

it follows that Eqs. (26(a))-(26(e)) read in matrix notation

$$\underbrace{\begin{bmatrix} \hat{w}_1(0) & \hat{w}_2(0) & \hat{w}_3(0) & \hat{w}_4(0) & \hat{w}_5(0) \\ \hat{w}_{1,x}(0) & \hat{w}_{2,x}(0) & \hat{w}_{3,x}(0) & \hat{w}_{4,x}(0) & \hat{w}_{5,x}(0) \\ \hat{w}_{1,xx}(l) & \hat{w}_{2,xx}(l) & \hat{w}_{3,xx}(l) & \hat{w}_{4,xx}(l) & \hat{w}_{5,xx}(l) \\ \hat{w}_{1,xx}(l) & \hat{w}_{2,xx}(l) & \hat{w}_{3,xx}(l) & \hat{w}_{4,xx}(l) & \hat{w}_{5,xx}(l) \\ r_1 & r_2 & r_3 & r_4 & p_z / P_z + r_5 \end{bmatrix}}_{\mathbf{W}} \underbrace{\begin{bmatrix} A_{w,1} \\ A_{w,2} \\ A_{w,3} \\ A_{w,4} \\ A_{w,5} \end{bmatrix}}_{\mathbf{A}} = \underbrace{\begin{bmatrix} 0 \\ 0 \\ 0 \\ 0 \\ p_z / P_z \end{bmatrix}}_{\mathbf{P}} \tag{29}$$

where the weighted volume displacement is defined as

$$r_j := \int_0^l \hat{w}_{j,xx}(x) b_p(x) dx \quad \text{for } j = 1, 2, \dots, 5. \tag{30}$$

If the impedance matching condition in Eq. (13) is met for a specific target frequency

$$P_z \rightarrow \infty \Rightarrow \mathbf{P} \rightarrow 0 \tag{31}$$

follows. Since the matrix W has full rank and is invertible, the coefficients converge to zero in the limit case

$$\mathbf{A} \rightarrow 0 \quad (32)$$

thus the vertical displacement field vanishes along the beam axis,

$$\hat{w}_0(x) \rightarrow 0 \quad x \in (0, l) \quad (33)$$

5. Case study: Smart passive cantilever beam excited by a triangular load and an end moment

As a structural example, we consider the cantilever depicted in Fig. 2. A time-harmonic linearly decreasing mechanical load along the beam axis $\hat{f}_z(x) = 1000 \cdot (1-x/l)e^{j\omega t}$ and a single moment $\hat{M}_0 e^{j\omega t}$ at the location $x = x_{M_0}$ (close to the free end) serve as external loads. In order to demonstrate the correctness of our derived conditions for the total vanishing of bending vibrations at a specific frequency, we compare a finite element code self-written in MATLAB with three-dimensional finite element calculations performed with ANSYS 11.0, using volume elements. Our objective is to nullify vibrations close to the first resonance frequency, which is about $f_1 = 75$ Hz for an open-circuited smart beam. The material for the substrate and the piezoelectric layer is aluminium and PZT-5A, respectively. The geometrical dimensions and the material properties of the example are summarized in Table 1.

The shaping condition Eq. (17) states that the contour of the layers and its spatial derivative must be proportional to the first and second antiderivative of the force loading, thus

$$\int_0^x \hat{q}_z(x) dx = -1000 \cdot \frac{(1-x/l)^2 l}{2} + \hat{M}_0 \delta(x - x_{M_0}) + G_{z,1} \propto b_{p,x}(x) \quad (34)$$

$$\int_0^x \int_0^x \hat{q}_z(x) dx dx = 1000 \cdot \frac{(1-x/l)^3 l^2}{6} + \hat{M}_0 H(x - x_{M_0}) + G_{z,1}x + G_{z,2} \propto b_p(x)$$

must hold. Because of the free end at $x = l$ (homogeneous natural boundary conditions), we apply Eq. (20).

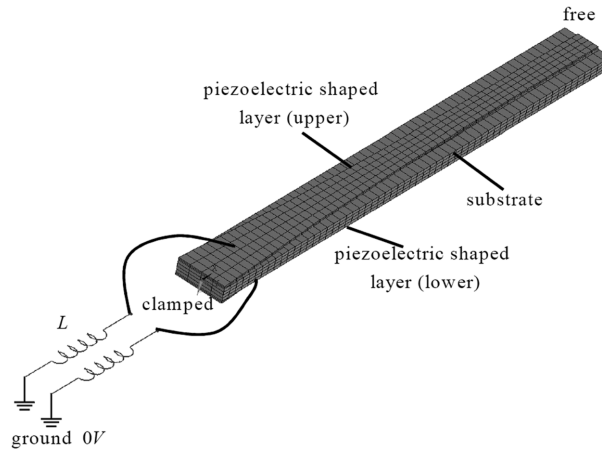


Fig. 2 Three dimensional finite element model of a smart clamped-free beam with attached inductive circuits. The electroded lower and upper layers are chosen according to Eq. (37)

Table 1 Numerical values for the case study

variable (unit)	value	variable (unit)	value
ρ_p (kgm ⁻³)	7750	ρ_p (kgm ⁻³)	2700
$z_{1,p}$ (m)	$5.00 \cdot 10^{-3}$	$z_{2,p}$ (m)	$7.00 \cdot 10^{-3}$
$z_{1,s}$ (m)	0	$z_{2,s}$ (m)	$5.00 \cdot 10^{-3}$
l (m)	0.4	f_1 (Hz)	75
$\tilde{\kappa}_{33}^p$ (AsV ⁻¹ m ⁻¹)	$2.10 \cdot 10^{-8}$	$\tilde{\epsilon}_{31}^p$ (Asm ⁻²)	-10.4827
\tilde{C}_{11}^p (Nm ⁻²)	$6.15 \cdot 10^{10}$	$\hat{f}_z(x)$ (Nm ⁻¹)	$1-x/l$
\hat{M}_0 (Nm)	-10	x_{M_0} (Nm)	0.4
b_s (m)	0.04	C_p (AsV ⁻¹)	$7.64 \cdot 10^{-8}$
L (VsA ⁻¹)	58.97		

$$b_p(l) = b_{p,x}(l) = 0 \quad (35)$$

hence both unknowns $G_{z,1}$ and $G_{z,2}$ can be specified according to Eq. (34), yielding

$$b_p(x) \propto 1000 \cdot \frac{(1-x/l)^3 l^2}{6} - \hat{M}_0 H(x_{M_0} - x) \quad (36)$$

This result can be nicely interpreted: the width is proportional to the quasi-static bending moment distribution caused by the external forces. Inserting the parameters listed in Table 1, we obtain the following distribution of the layers

$$b_p(x) = 0.0291 \cdot (1-x/0.4)^3 + 0.0109 H(x_{M_0} - x) \quad (37)$$

where $b_s = b_p(0) = 0.04$ is assumed to be the maximum width. If capacitive effects of the electric circuit are neglected $C \rightarrow \infty$, the inductance is specified by the impedance matching condition Eq. (14) for a target frequency $f_1 = 75$ Hz

$$L = \frac{1}{\omega_1^2 C_p} = 58.97 \text{H} \quad \text{where} \quad C_p = \int_0^l \frac{\tilde{\kappa}_{33}^p b_p(x) dx}{z_{2,p} - z_{1,p}} = 7.64 \cdot 10^{-8} \text{AS/V} \quad (38)$$

The finite element model (ANSYS) is depicted in Fig. 2. The substrate and two piezoelectric layers are divided into 60 and 4 elements along the x - and y -axis, respectively. In thickness direction the substrate and the layers are built up by 4 and 2 elements. A three-dimensional coupled-field solid element called SOLID5 (three displacement and one electrical degree of freedom) is used, which optionally enables coupled field analysis between the mechanical and piezoelectric domain. The serial circuits are modeled by CIRCU94 elements which can be used for either resistive, inductive or capacitive impedances, or a combination of them. Ideal electrodes are modeled by coupling the electrical degrees of freedom at $z = \pm z_{2,s}$ and $z = \pm z_{2,p}$. The inner electrodes are grounded, the external ones are connected to the electric circuits. MATLAB R2006b is used for the self-written finite element code. The lateral equation of motion in Eq. (5) is discretized by 10 Bernoulli beam elements and considers the spatially nonlinear distribution of the layers. For both finite element models, a modal damping coefficient $d = 0.01$ is assumed. The value for the inductance L is chosen according to Eq. (38), the resistance and the capacitance are $R \rightarrow 0$ and $C \rightarrow \infty$, so practically an inductive network is obtained.

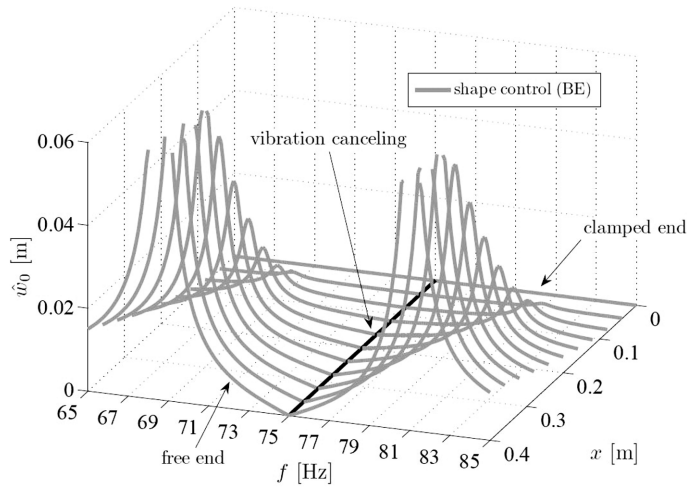


Fig. 3 Vibration suppression of the cantilever at $f_1 = 75$ Hz considered in this case study (Bernoulli-Euler finite elements)

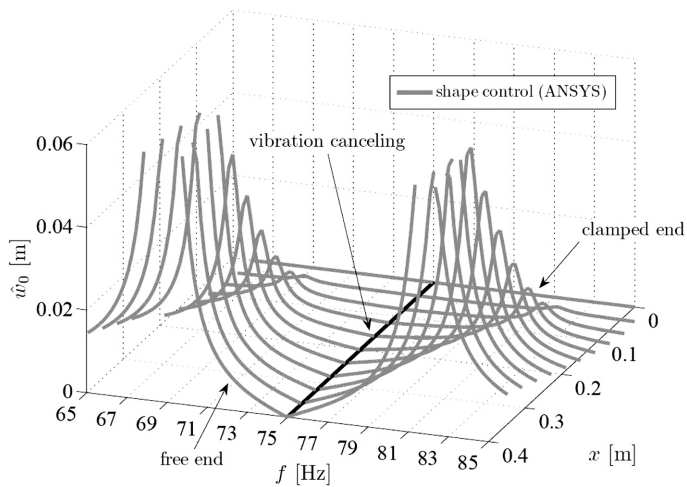


Fig. 4 Vibration suppression of the cantilever at $f_1 = 75$ Hz considered in this case study (ANSYS)

In Fig. 3 (Bernoulli-Euler finite elements) and Fig. 4 (ANSYS), the vertical deformation of the beam is shown as a function of the axial coordinate and the excitation frequency. In both cases we can observe that the deformation exactly vanishes at $f_1 = 75$ Hz (straight black line). This means that no point along the beam axis vibrates: at every point on the x -coordinate the external force is in equilibrium to the equivalent electric circuit force whose intensity is proportional to second derivative of the width of the layers. If one only fulfills the impedance condition and violates the shaping condition (e.g., two uniformly distributed layers), one would not obtain a straight, but a curved black line in the f - x plane (frequency-axial coordinate): This means that the transmission zeros of the tip deflection are frequency dependent. It can be shown by parametric studies that the higher the electromechanical coupling $\tilde{e}_{31}^2(\tilde{C}_{11}\tilde{\kappa}_{33})^{-1}$ is, the more important is an optimal and robust controller design concerning the width of the layers. The optimization of the electrical parameters and mechanical parts of the beam (e.g., the width) is a topic of current interest, since the variation of

Table 2 Comparison of the natural frequencies of the smart passive cantilever for different electrical boundaries (short-, open- and optimally tuned inductive circuit with L specified by Eq. (38)) with Bernoulli-Euler (BE) and three-dimensional solid finite elements (ANSYS) (Hz)

mode	short-circuit		open-circuit		ind. circuit	
	BE	ANSYS	BE	ANSYS	BE	ANSYS
f_1	74.29	74.92	75.32	75.96	68.63	69.55
f_{el}	-	-	-	-	81.05	81.75
f_2	424.98	424.86	425.09	424.97	425.09	424.97
f_3	1157.9	1147.1	1158.5	1147.7	1158.5	1147.7
f_4	2252.9	2206.5	2253.3	2206.8	2253.3	2206.8

one parameters may easily have impacts on the others. Additionally, Table 2 compares the eigenfrequencies of the ANSYS and BE finite elements results confirming the correctness of the derived one-dimensional electromechanically coupled theory. As expected, the short-circuit eigenfrequencies are lower than the open-circuited ones. If an inductance is added to the electric circuit, the network is strongly coupled to the first structural eigenmode and therefore two eigenfrequencies f_1 and f_{el} occur in the lower frequency domain. One can see that our BE-FE results are in a good coincidence with the results from the commercial FE-code. For the higher modes, the BE-FE values are higher since the shear deformation and rotary inertia are neglected.

Fig. 5 shows an alternative illustration, where the deflections for $x = 0.3l$, $x = 0.5l$ and $x = l$ are drawn. The three pictures at the top part are obtained from our one-dimensional theory, the figures at the bottom are the ANSYS results. The short- and open-circuited deformations are shown by the light and dark gray lines, whereas the deformations according to the shape control theory are the black lines. For the inductive circuit, the magnitude of vibration is zero at $f_1 = 75$ Hz. One can see

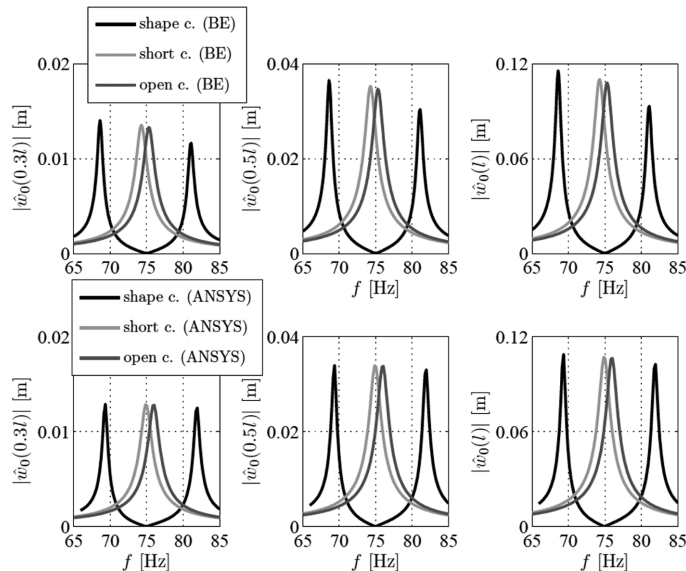


Fig. 5 Frequency response \hat{w}_0 of the beam close to the first structural natural eigenfrequency at three different locations $x = 0.3l$ (left), $x = 0.5l$ (middle) and $x = l$ (right), shown for a short- and open-circuited and an optimally tuned beam (above: results from self-written BE-FE code, below: ANSYS results)

that the one- and three-dimensional results only slightly differ, confirming the correctness of the beam theory for smart passive beams and validating the correctness of the passive shape control theory, even if mechanical damping is taken into account in terms of modal damping.

6. Practical application of the shape control theory

One of the main disadvantages of passive vibration control by means of inductive circuits is the high sensitivity to parameter uncertainties, mainly caused by the small electromechanical coupling factor $\tilde{e}_{31}^2(\tilde{C}_{11}\tilde{\kappa}_{33})^{-1}$. This coefficient only depends on the material properties and is a measure for the energy relocation between mechanical and electrical domain. Often real applications show a broadband frequency content of the excitation signals or the material parameters are time-variant, so resistive-inductive networks are an alternative choice for passive vibration control in practice. It is however not possible, to realize the above goal of complete cancelation with $R \neq 0$.

In this section, we will optimize the dissipative and inductive parts of the circuit by minimizing the tip deflection around the first structural peak (frequencies from 0 to 100 Hz)

$$\min_{\omega \in (0, 2\pi \cdot 100)} \|\hat{w}_0(l, \omega)\| \quad \text{w.r.t. } R, L. \quad (39)$$

We consider two different beam configurations and prescribe the same transversal load as in the case study previously discussed. The geometrical dimensions and the material properties are also given in Table 1. For the first configuration, the layer distribution is determined by the shape control theory (resulting in the same shaped layer width as before, see Eq. (37)). For the second beam, we assume that two uniformly distributed layers are attached to the upper and lower surface of the substrate. The mean width of these layers is obtained from Eq. (37) by integrating the layer width and by dividing through the length of the beam

$$\bar{b}_p = \frac{1}{l} \int_0^l 0.0291 \cdot (1 - x/0.4)^3 + 0.0109H(x_{M_0} - x) dx \approx 0.01818\text{m} \quad (40)$$

Consequently the area of electrodes and the piezoelectric capacitance are the same for both beams. Since the width of the layers changes the mass and stiffness properties of the layer Eq. (6), causing different eigenfrequencies for both beam versions, we simply neglect these effects by setting

$$M_w \approx \rho_s b_s (z_{2,s} - z_{1,s}), K_M \approx \tilde{C}_{11}^s b_s \frac{z_{2,s}^3 - z_{1,s}^3}{3} \quad (41)$$

We note that this simplification is only an approximation of our numerical example, but it is a reasonable choice since we intend to point out the influence of the layer distribution and the RL -optimized circuit alone. Both beam configurations are discretized by 10 Bernoulli-Euler beam elements and the mechanical modal damping is assumed to be $d = 0.01$ again. The final results are given by Figs. 6 and 7. Fig. 6 shows the deflections for frequencies between 53 and 73 Hz, for a passive smart beam with short- and open-circuited electrodes (black and light gray) and with an optimized electric circuit. The left and right pictures belong to the beam with the shaped and constant piezoelectric layers, respectively. The curves for the short-circuited beams (black) are the same in both cases, since the inertia and the bending stiffness of the layers are neglected. But the influence of the electric circuit is a bit more dominant for the beam with varying layers: the eigenfrequency for an open-circuit is higher

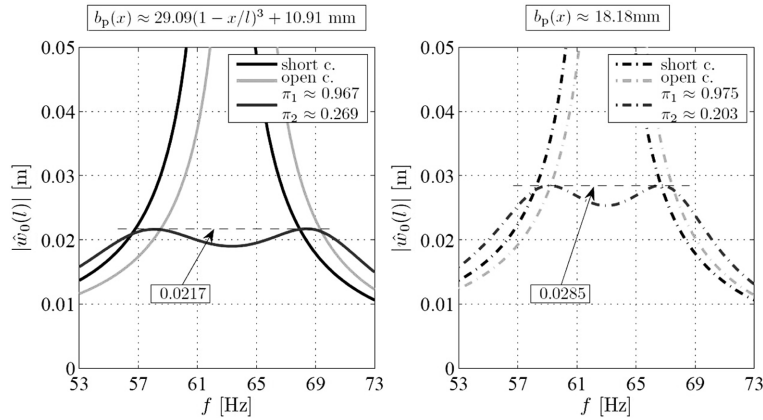


Fig. 6 Reduction of harmonic vibrations using an RL -optimized network with different layer contours (left: shaped layers as a result of the shape control theory with $\pi_1 = 0.967$ and $\pi_2 = 0.269$, right: layers with uniform width \bar{b}_p and $\pi_1 = 0.975$ and $\pi_2 = 0.203$).

64.2 Hz > 63.6 Hz, since the circuit and the width influence the beam stiffness (see the third term in Eqs. (5) and (7)). In order to minimize Eq. (39), the values for the inductance and the resistance are varied. The maximal deflection over the considered frequency range is decreased from 0.0285m to 0.0217m (reduction of about -24%), demonstrating the ability of shaped layers to bring more electrical damping into the mechanical part of the system. A local minimum of the vibration occurs at $f_1 \approx 63$ Hz for both beams, therefore one may define the dimensionless impedances $\pi_1 := \omega_1^2 C_p L$ and $\pi_2 := \omega_1 C_p R$

$$\begin{aligned} \text{shaped layers: } L = 80.5\text{H}, R = 8856\Omega &\Leftrightarrow \pi_1 = 0.967, \pi_2 = 0.269 \\ \text{constant layers: } L = 81.2\text{H}, R = 6693\Omega &\Leftrightarrow \pi_1 = 0.975, \pi_2 = 0.203 \end{aligned} \quad (42)$$

A parametric study shows that if the modal damping coefficient of the mechanical part is even lower

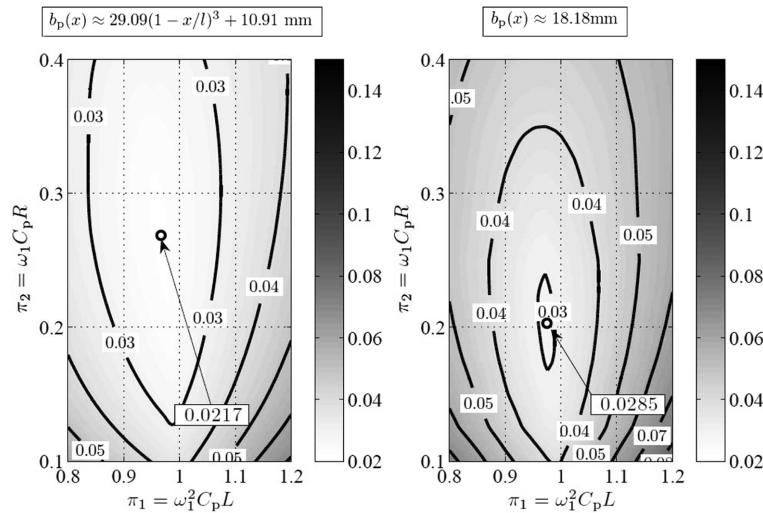


Fig. 7 Contour plot of the maximum tip deflections around the structural eigenfrequency as a function of the dimensionless inductance π_1 and resistance π_2 (left: shaped layers, right: layers with uniform width)

than $d = 0.01$, the relative reduction of the deflection can be significantly increased. Fig. 7 shows a contour plot, where the maximum deflection over the considered frequency range is a function of the dimensionless inductance π_1 and resistance π_2 . The minimum deflection is marked by the two black circles (0.0217 m and 0.0285 m). This figure gives a good overview of the robustness and sensitivity of the electrical parameters. The background color of the shaped layer configuration is much lighter and the contour ellipses are larger, meaning that the sensitivity of the beam with distributed layers is much lower than in the other case. This is an important topic in control engineering when dealing with uncertain elements in physical models, where advanced robust control methods are used (H_∞ and H_2 -controllers).

7. Conclusions

In the present paper, necessary and sufficient conditions have been derived in order to nullify harmonic deflections of a transversally excited electromechanically coupled Bernoulli-Euler beam at any point along the axial coordinate by means of passive vibration control. This aim is achieved if the shape of the piezoelectric layers is proportional to the the quasi-static bending moment due to the external forces, and if the electrical eigenfrequency is equal to the excitation frequency of the external load. For a slender clamped-free beam which is exposed to a time-harmonic triangular load and an end moment, the correctness of the proposed method is verified by a three-dimensional electromechanically coupled finite element calculation performed with ANSYS 11.0. The practical importance of the spatial distribution of the piezoelectric layers is shown if vibrations should be suppressed by an RL -networks. The magnitude of deflections around the first eigenfrequency of a smart passive beam with a layer distribution according to the shape control theory is reduced by one quarter compared to a beam with uniformly distributed layers. Further research activities concerning the simultaneous optimization of the connected network and the shape of the electrodes, taking into account uncertain parameters and robustness, seem to be necessary. However, these procedures will require more complex mathematical optimization approaches, but this topic is of high practical interest and is planned to be studied in the future.

Acknowledgements

Support of the authors J. Schoeftner and H. Irschik by the Austrian Center of Competence in Mechatronics (ACCM) is gratefully acknowledged.

References

- Behesthi-Aval, S.B. and Lezgy-Nazargah, M. (2010), "Assessment of velocity-acceleration feedback in optimal control of smart piezoelectric beams", *Smart Struct. Syst.*, **6**(8), 921-38.
- Benjeddou, A. (2009), "New insights in piezoelectric free-vibrations using simplified modeling and analyses", *Smart Struct. Syst.*, **5**(6), 591-612.
- Gabbert, U., Nestorovic, T. and Wuchatsch, J. (2007), "Methods and possibilities of a virtual design for actively controlled smart systems", *Comput. Struct.*, **86**(3-5), 240-50.
- Hafka, R.T. and Adelman, H.M. (1985), "An analytical investigation of shape control of large space structures by

- applied temperatures”, *AIAA J.*, **23**(3), 450-57.
- Hubbard, J.E. and Burke, S.E. (1992), *Distributed transducer design for intelligent structural components*, in: *Intelligent Structural System*, (Eds. H.S. Tzou and G.L. Anderson), Kluwer Academic Publishers, Norwell.
- Irschik, H. (2002), “A review on static and dynamic shape control of structures by piezoelectric actuation”, *Eng. Struct.*, **24**(1), 5-11.
- Irschik, H., Krommer, M., Belayaev, A.K. and Schlacher, K. (1998), “Shaping of piezoelectric sensors/actuators for vibrations of slender beams: coupled theory and inappropriate shape functions”, *J. Intell. Mater. Syst. Struct.*, **9**(7), 546-54.
- Irschik, H., Krommer, M. and Pichler, U. (2001), “Collocative control of beam vibrations with piezoelectric self-sensing layers”, (Eds. U. Gabbert and H.S. Tzou), *Proceedings of the IUTAM Symposium on Smart Structures and Strucronic Systems*, Magdeburg, Kluwer Academic Publisher.
- Irschik, H., Krommer, M. and Pichler, U. (2003), “Dynamic shape control of beam-type structures by piezoelectric actuation and sensing”, *Int. J. Appl. Electrom.*, **17**(1-3), 251-58.
- Irschik, H. and Pichler, U. (2004), “An extension of Neumann’s method for shape control of force-induced elastic vibrations by eigenstrains”, *Int. J. Solids Struct.*, **41**(3-4), 871-84.
- Krommer, M. (2001), “On the correction of the Bernoulli-Euler beam theory for smart piezoelectric beams”, *Smart Mater. Struct.*, **10**(4), 668-80.
- Krommer, M. (2005), “Dynamic shape control of sub-sections of moderately thick beams”, *Comput. Struct.*, **83**(15-16), 1330-39.
- Krommer, M. and Irschik, H. (2002), “An electromechanically coupled theory for piezoelastic beams taking into account the charge equation of electrostatics”, *Acta Mech.*, **154**(1-4), 141-58.
- Nader, M. (2007), *Compensation of Vibrations in Smart Structures: Shape Control, Experimental Realization and Feedback Control* (Doctoral thesis Johannes Kepler Universitaet Austria), Trauner Verlag, Linz.
- Nader, M., Gattringer, H., Krommer, M. and Irschik, H. (2003), “Shape control of flexural vibrations of circular plates by shaped piezoelectric actuation”, *J. Vib. Acoust.*, **125**(1), 88-94.
- Nitzsche, F. and Breitbach, E. (1994), “Vibration control of rotary wings using smart structures”, *Smart Mater. Struct.*, **3**(2), 181-89.
- Schoeftner, J. and Irschik, H. (2009), “Passive damping and exact annihilation of vibrations of beams using shaped piezoelectric layers and tuned inductive networks”, *Smart Mater. Struct.*, **18**(12), 125008.
- Schoeftner, J. and Irschik, H. (2010), “Piezoelastic structures interacting with electric networks: vibration canceling and shape control”, *Proceedings of the 5th World Conference on Structural Control and Monitoring*, Tokyo, July.
- Yu, Y., Zhang, X.N. and Lie, S.L. (2009), “Optimal shape control of a beam using piezoelectric actuators with low control voltage”, *Smart Mater. Struct.*, **18**(9), 095006.
- Zehetner, C. (2010), *Piezoelectric Compensation of Flexural and Torsional Vibrations in Beams Performing Rigid Body Motions* (Doctoral thesis Johannes Kepler Universitaet Austria), Trauner Verlag, Linz.
- Zehetner, C. and Irschik, H. (2008), “On the static and dynamic stability of beams with an axial piezoelectric actuation”, *Smart Struct. Syst.*, **4**(1), 67-84.
- Zhou, Y.G., Chen, Y.M. and Ding, H.J. (2005), “Analytical solutions to piezoelectric bimorphs based on improved FSDT beam model”, *Smart Struct. Syst.*, **1**(3), 309-324.
- Ziegler, F. (1995), *Mechanics of Solids and Fluids*, 2nd Ed., Springer Verlag, New York.
- Ziegler, F. (2005), “Computational aspects of structural shape control”, *J. Sound Vib.*, **83**(15-16), 1191-1204.